EUKARYOTIC CELL, May 2011, p. 646–653 Vol. 10, No. 5
1535-9778/11/$12.00 doi:10.1128/EC.00304-10

Quantifying the Importance of Galactofuranose in *Aspergillus nidulans* Hyphal Wall Surface Organization by Atomic Force Microscopy▽†

Biplab C. Paul,[1]‡ Amira M. El-Ganiny,[2,3]‡ Mariam Abbas,[1]
Susan G. W. Kaminskyj,[2]§ and Tanya E. S. Dahms[1]§*

Department of Chemistry and Biochemistry, University of Regina, 6262 Wascana Parkway, Regina, SK S2S 0A2, Canada[1]; Department of Biology, University of Saskatchewan, 112 Science Place, Saskatoon, SK S7N 5E2, Canada[2]; and Microbiology Department, Faculty of Pharmacy, Zagazig University, Zagazig, Egypt[3]

Received 3 December 2010/Accepted 14 February 2011

The fungal wall mediates cell-environment interactions. Galactofuranose (Gal*f*), the five-member ring form of galactose, has a relatively low abundance in *Aspergillus* walls yet is important for fungal growth and fitness. *Aspergillus nidulans* strains deleted for Gal*f* biosynthesis enzymes UgeA (UDP-glucose-4-epimerase) and UgmA (UDP-galactopyranose mutase) lacked immunolocalizable Gal*f*, had growth and sporulation defects, and had abnormal wall architecture. We used atomic force microscopy and force spectroscopy to image and quantify cell wall viscoelasticity and surface adhesion of *ugeA*Δ and *ugmA*Δ strains. We compared the results for *ugeA*Δ and *ugmA*Δ strains with the results for a wild-type strain (AAE1) and the *ugeB* deletion strain, which has wild-type growth and sporulation. Our results suggest that UgeA and UgmA are important for cell wall surface subunit organization and wall viscoelasticity. The *ugeA*Δ and *ugmA*Δ strains had significantly larger surface subunits and lower cell wall viscoelastic moduli than those of AAE1 or *ugeB*Δ hyphae. Double deletion strains (*ugeA*Δ *ugeB*Δ and *ugeA*Δ *ugmA*Δ) had more-disorganized surface subunits than single deletion strains. Changes in wall surface structure correlated with changes in its viscoelastic modulus for both fixed and living hyphae. Wild-type walls had the largest viscoelastic modulus, while the walls of the double deletion strains had the smallest. The *ugmA*Δ strain and particularly the *ugeA*Δ *ugmA*Δ double deletion strain were more adhesive to hydrophilic surfaces than the wild type, consistent with changes in wall viscoelasticity and surface organization. We propose that Gal*f* is necessary for full maturation of *A. nidulans* walls during hyphal extension.

The fungal wall supports and shields the hyphal cytoplasm and mediates interactions between the cell and its environment. Fungal walls are typically about 30% of the weight (dry weight) of the cell (7, 10), and a similar portion of the fungal genome is thought to contribute to cell wall biosynthesis and/or maintenance (11, 17). Fungal walls are composed of a variety of carbohydrate polymers (7, 11, 15); however, deleting many wall biosynthesis genes appears to be compensated by genetic redundancy and/or by induction of the cell wall integrity pathway (6, 7, 23).

The *Aspergillus* wall is reinforced by chitin fibrils and has a matrix containing alpha- and beta-glucans, other sugars, including galactomannans, and proteins. Galactofuranose (Gal*f*) is the five-member ring form of galactose that is found in the cell walls of *Aspergillus* spp. (6, 7, 23), other fungi (reviewed in reference 15), and certain other microbes (3). Deletion of UDP-galactopyranose mutase in several *Aspergillus* species has shown that Gal*f*, despite its reported low abundance, is important for wild-type fungal growth, cell morphogenesis, hyphal adhesion, wall architecture, and spore development (6, 8, 9, 14, 16, 25) and may mediate pathogenesis (1, 21–23).

The *A. nidulans* gene products UgeA (UDP-glucose-4-epimerase) (8), and UgmA (UDP-galactopyranose mutase) (9) catalyze sequential steps in Gal*f* biosynthesis (Fig. 1). The *ugeA*Δ and *ugmA*Δ deletion strains have similarly compact colonies, aberrant hyphal growth, and reduced sporulation. The hyphal walls of these strains differ from those of the wild type and from each other as visualized using transmission electron microscopy (TEM) (8).

Atomic force microscopy (AFM) imaging uses a fine-tipped probe mounted on a flexible cantilever to raster scan the surface of an object generating a topographic map. An approach-retract cycle of the AFM probe, called force spectroscopy (FS), can be used to calculate the viscoelastic modulus of the whole organism or its cell surface and surface adhesion. Previously we used AFM to show that *A. nidulans* cell walls of growing hyphal tips differ from those of mature regions (18) and to document changes associated with spore swelling and germination and the nonpolarized hyphal growth of temperature-sensitive mutants (19). Here, we compare the hyphal walls of the wild type and a suite of Gal*f* biosynthesis gene deletion strains using TEM, AFM, and FS to gain a better understanding of the role played by Gal*f* in *Aspergillus nidulans* cell wall organization.

MATERIALS AND METHODS

Strains and culture conditions. *Aspergillus nidulans* strains were grown as described in references 8 and 9. Deletion strain construction followed procedures described in references 8 and 9 using *nkuA*Δ strains, plasmids, and primers listed in Table SA in the supplemental material. The AN2951 (*ugeB*) gene was deleted

* Corresponding author. Mailing address: Department of Chemistry and Biochemistry, University of Regina, 6262 Wascana Parkway, Regina, SK S2S 0A2, Canada. Phone: (306) 585-4246. Fax: (306) 337-2409. E-mail: tanya.dahms@uregina.ca.

† Supplemental material for this article may be found at http://ec.asm.org/.

‡ These two authors contributed equally to the research in this article.

§ These two authors contributed equally to writing this article.

▽ Published ahead of print on 18 February 2011.

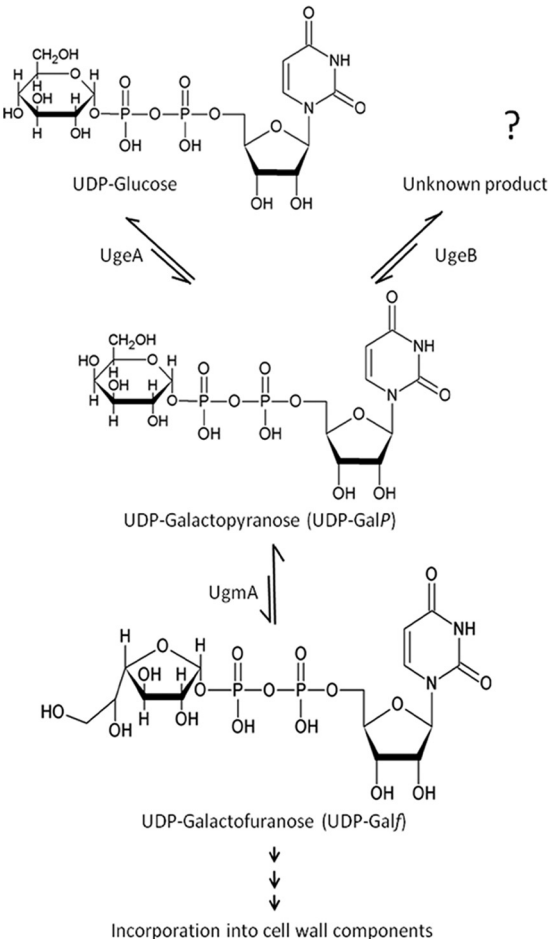

FIG. 1. Biosynthesis of galactofuranose (Gal*f*) from UDP-glucose. UDP-glucose is converted to UDP-galactopyranose by UDP-glucose-4-epimerase (UgeA). In the reaction shown, UDP-galactopyranose is converted to the final product UDP-galactofuranose by UDP-galactopyranose mutase (UgmA). These two enzymes are localized in the cytoplasm, and then UDP-galactofuranose is transported to the fungal Golgi equivalent, which is the site of incorporation into other cell wall components.

from strain A1149 using *Aspergillus fumigatus pyroA* (*AfpyroA*) as the selectable marker (amplified from pTN1) to generate strain AAE9. The *ugeA* gene was then deleted from strain AAE9 using *AfpyrG* as the selectable marker (amplified from pAO18) to create the *ugeA*Δ *ugeB*Δ double deletion strain AAE10. Construction of strain AAE8 (*ugeA*Δ *ugmA*Δ double deletion strain) was described in reference 8. All *Aspergillus nidulans* strains were cultured in either liquid or solid complete medium (CM) as described in reference 13.

One liter of complete medium (CM) contains 10 g D-glucose, 2 g peptone, 1 g yeast extract, 1 g Casamino Acids, 50 ml of 20× nitrate salts (formulation follows), 1 ml trace elements (formulation follows), and 1 ml of vitamin solution (formulation follows). The pH of the CM was adjusted to pH 6.5 with KOH solution. When required, CM was solidified with 18 g/liter Bacto agar. One liter of the 20× nitrate salts solution contains 120 g $NaNO_3$, 10.4 g KCl, 10.4 g $MgSO_4 \cdot 7H_2O$, and 30.4 g KH_2PO_4. One hundred milliliters of trace element solution contains 2.2 g $ZnSO_4 \cdot 7H_2O$, 1.1 g H_3BO_3, 0.5 g $MnCl_2 \cdot 4H_2O$, 0.5 g $FeSO_4 \cdot 7H_2O$, 0.17 g $CoCl_2 \cdot 6H_2O$, 0.16 g $CuSO_4 \cdot 5H_2O$, 0.15 g $Na_2MoO_4 \cdot 2H_2O$, and 5 g Na_4EDTA. The pH of the trace elements solution was adjusted to pH 6.5 with KOH. One hundred milliliters of vitamin solution contains 100 mg each of biotin, pyridoxin, thiamine, riboflavin, *p*-aminobenzoic acid, nicotinic acid, and 2 drops of chloroform added as a preservative. The vitamin solution was stored in a dark bottle, since riboflavin is light sensitive. The 20× nitrate salts, trace elements, and vitamin solutions were autoclaved for 20 min at 121°C, cooled to room temperature, and then stored at 4°C. For growth of *A. nidulans* auxotrophic strains (see Table SA in the supplemental material), CM was supplemented with the appropriate nutrient as described in reference 13.

Confocal fluorescence and transmission electron microscopy (TEM). Samples were prepared for confocal microscopy as described in reference 9. Briefly, freshly harvested spores were grown on coverslips for 16 h at 28°C in liquid complete medium, fixed, stained with Hoechst 33258 (for nuclei) or Calcofluor (for cell walls), and then imaged by confocal microscopy. Hyphal width and basal cell length were measured at septal positions in mature regions (~40 μm from the tip) for 50 cells per strain using LSM examiner.

For TEM, wild-type and gene deletion strains were grown on dialysis tubing laid over complete medium agar for 1 day at 28°C and then fixed, embedded, and sectioned as described previously (9). Hyphal wall thickness was measured on TEM cross sections of 10 hyphae per strain, typically three measurements per hypha, at places where the cell membrane was crisply focused.

AFM. Samples for imaging fixed hyphae were prepared for atomic force microscopy (AFM) as previously described (18, 19). Briefly, conidia were germinated in liquid growth medium between two glass coverslips for 16 h. The top coverslip was carefully removed, and the hyphae were fixed with 3.7% formaldehyde in 50 mM phosphate buffer (pH 7.0) containing 0.2% Triton X-100, followed by rinsing with distilled water and air drying. For live-cell AFM imaging, hyphae were grown on dialysis tubing (Spectrapor; 12 to 14 kDa) overlaying agar medium. After 16 h of growth, the dialysis tubing was transferred to a glass coverslip. Sterile Whatman no. 4 filter paper placed beneath the dialysis tubing was used to deliver liquid growth medium by capillary action, ~20 μl at a time.

An Explorer AF microscope (Veeco, Plainview, NY) with a dry scanner (model 5460-00; Veeco) was used for contact mode imaging and force spectroscopy (FS), as previously described (18, 19). Hyphae were visualized by using a charge-coupled-device (CCD) camera (magnification of ×200) and imaged first at low resolution (200 by 200 lines per scan). All topographic and lateral force data were collected from high-resolution images (500 by 500 lines per scan) of fixed and live cells (scan rate of 1 and 2 Hz, respectively) using Si_3N_4 probe tips (model 1520-00 [Veeco]; $k = 0.05$ nN/nm; nominal resonance $n = 17$ kHz). The images shown are typical results. AFM tip size and shape were calibrated using gold spheres according to reference 27.

FS. Cantilever spring constants, k_c, were determined prior to each force measurement using resonance frequencies according to reference 5. Tip-sample interaction was tracked by cantilever deflection as a function of Z piezo elongation during probe approach and retraction. For soft materials, meaningful FS comparisons often depend on the velocity of the surface approach (4). In this case, the approach velocity did not significantly affect the hyphal spring constant (data not shown), but this parameter was kept constant (100 nm/s) to facilitate comparison of viscoelastic moduli between samples. Repeated measurements of individual sites on mature walls gave consistent values, and images obtained before and after FS were unchanged (data not shown), indicating that the walls were not damaged during data collection. Values were averaged from force curves collected in triplicate at 10 separate points on the surfaces of mature hyphal walls (≥40 μm from the tip) for five hyphae per sample and typically three different samples.

Force approach curves measure the unit force (in nanonewtons) required to indent a surface a given distance (in nanometers), so the slope corresponding to the b-c segment of the approach cycle (see Fig. 5A) was used to examine the relative cell wall elasticity. FS data were plotted as deflection (in nanoamperes) versus distance (in nanometers), converted to force (in nanonewtons) versus distance (in nanometers) curves using the piezo sensor response, and the slope of the line b-c (m) in nanonewtons per nanometer used to determine the spring constant k_w of the cell wall according to the following equation:

$$k_w = m_s k_c / (m_h - m_s) \quad (1)$$

where m_s is the sample slope and m_h is the slope for a hard surface (mica). The value of k_w was used for the subsequent determination of Young's modulus according to the following equation (28):

$$E = 0.80\,(k_w/h)(R/h)^{1.5} \quad (2)$$

where E is the cell wall viscoelastic (Young's) modulus, R is the hyphal radius measured by either TEM or AFM, and h is the thickness of the cell wall measured by TEM. Surface adhesion values were measured from the last segment of the retraction cycle (see Fig. 5A, segment e-f). If there is a chemical attraction between the sample and the Si_3N_4 AFM probe, which is hydrophilic, segment e-f will be a measure of its intensity in nanonewtons.

Data processing and analysis. AFM images were processed using horizontal leveling, with the maximal height adjusted for optimum contrast (SPMLab ver-

sion 6.0 software; Veeco). Hyphal widths at mature regions (~40 μm from the tip) and surface feature dimensions from topography and lateral force images were measured at the full width at half maximum of the peak height. AFM data are presented as means ± standard deviations or as ranges of values. TEM and confocal microscopy data are presented as means ± standard errors of the means. Differences in the mean subunit sizes of wild-type and deletion strain hyphae were tested by a one-way analysis of variance (ANOVA) (InStat 3; GraphPad Prism). Propagated errors were calculated for viscoelastic moduli based on equations 1 and 2, and a Student's *t* test (two-tailed test) was used to assess significant differences in the values (InStat 3; GraphPad Prism).

RESULTS

Building on our previous experience using atomic force microscopy (AFM) to study *Aspergillus nidulans* hyphae (18, 19), we compared a suite of *A. nidulans* strains deleted for galactofuranose (Gal*f*) biosynthesis enzymes UgeA and UgmA, the near-isogenic wild-type strain AAE1, a strain deleted for an epimerase (UgeB) that did not affect hyphal morphogenesis, and double deletion strains (*ugeA*Δ *ugeB*Δ and *ugeA*Δ *ugmA*Δ). Double deletion strains were used to further explore the function of individual gene products. Even enzymes that mediate a known biochemical function may have collateral defects in a deletion strain based on protein-protein interactions, for example if the protein is part of a scaffold for a multienzyme.

Characterization of *Aspergillus nidulans ugeB*. *Aspergillus nidulans* ANID2951.4 (which we named UgeB) shares 38% amino acid sequence identity with UgeA (8) and had been annotated as a UDP-glucose/galactose-4-epimerase (www.broadinstitute.org/annotation/genome/aspergillus_group/). The *ugeB* genomic sequence has a single exon that encodes a 428-amino-acid peptide. The *ugeB* cDNA could not be amplified (three attempts), unlike *ugmA* (7) and *ugeA* (8). We deleted *ugeB* (see Fig. SA in the supplemental material) as described in reference 9 and confirmed the deletion using PCR (see Table SA and Fig. SA in the supplemental material). A *ugeA*Δ *ugeB*Δ double deletion strain was generated and confirmed (see Fig. SB in the supplemental material) as described in reference 8. The *ugmA*Δ single deletion strain was described in reference 9, and the *ugeA*Δ single deletion strain and *ugeA*Δ *ugmA*Δ double deletion strain were described in reference 8. UgeB was expressed *in vitro* using the genomic sequence, which does not contain introns, purified, and shown to convert UDP-galactose into a product that is not UDP-glucose by the procedure described in reference 8 (data not shown). This unknown product awaits conclusive identification.

The *ugeB* sequence was put under the control of the *alcA* promoter and tagged with red fluorescent protein (A. M. El-Ganiny and S. G. W. Kaminskyj, unpublished data) and then overexpressed by culturing on CM containing 100 mM threonine (CMT). Under these conditions, p*alcA-ugeB-rfp* was expressed, albeit weakly, in conidia and to a lesser extent in mature hyphae (see Fig. SC in the supplemental material), but it was not detectable in hyphal tips (data not shown).

Morphology of *Aspergillus nidulans* strains deleted for Gal*f* biosynthesis genes. Confocal microscopy images showing the hyphal morphology of the suite of Gal*f* biosynthesis gene deletion strains examined in this study (strain AAE1, *ugeA*Δ and *ugeB*Δ single deletion strains, *ugeA*Δ *ugeB*Δ double deletion strain, *ugmA*Δ single deletion strain, and *ugeA*Δ *ugmA*Δ double deletion strain) are shown in Fig. 2. Strain morphometry is described in Table 1. Unlike the previously described *ugeA*Δ and *ugmA*Δ deletion strains, which had wide and highly branched hyphae and reduced sporulation (8, 9), the *ugeB*Δ strain had wild-type hyphal morphology and growth rate and abundant sporulation (Table 1 and Fig. 2; also data not shown). The *ugeA*Δ *ugeB*Δ double deletion strain was viable when grown on medium containing glucose as the carbon source, but it did not form colonies on medium containing galactose as the sole carbon source (due to *ugeA*Δ), and its hyphae were wide and branched like those of *ugeA*Δ (Table 1 and Fig. 2).

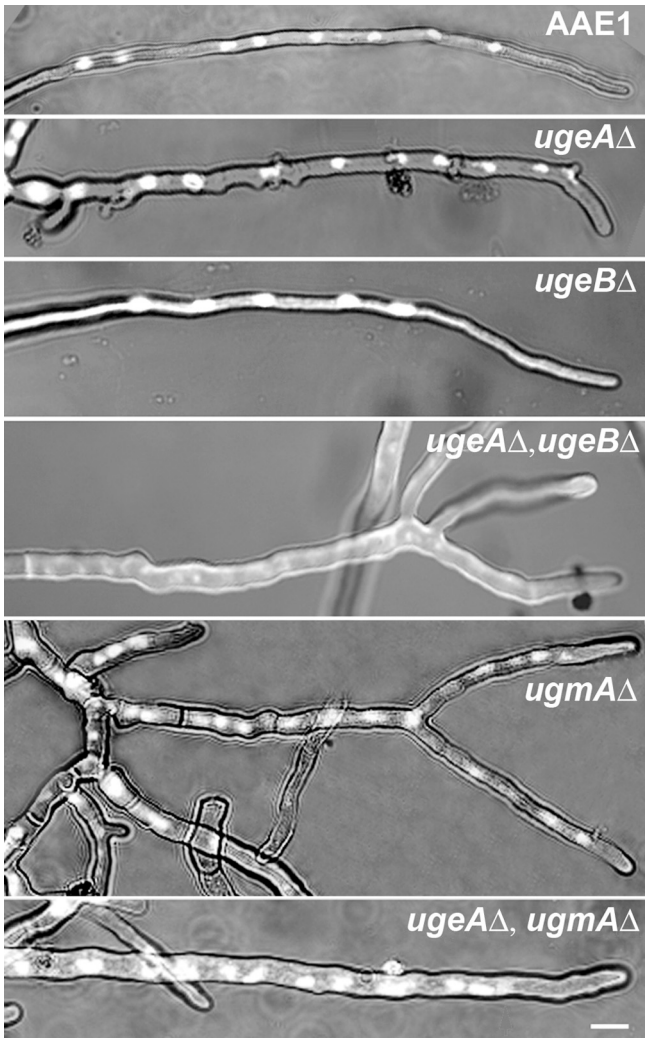

FIG. 2. Appearance of the hyphae of wild-type and Gal*f* biosynthesis gene deletion strains used in this study. Wild-type strain AAE1, *ugeA*Δ and *ugeB*Δ single deletion strains, *ugeA*Δ *ugeB*Δ double deletion strain, *ugmA*Δ single deletion strain, and *ugeA*Δ *ugmA*Δ double deletion strain were examined. The strains were grown for 16 h, then fixed, and stained with Hoechst 33258 to visualize nuclei. Images are combined fluorescence and transmitted light images. All images were photographed at the same magnification. Bar = 5 μm.

Transmission electron micrographs of hyphal cross sections showed that the walls of *ugeA*Δ and *ugmA*Δ single deletion strains were 2-fold and 4-fold thicker, respectively, than those of strain AAE1 (Table 1 and Fig. 3) (8, 9). Given the general correlation between hyphal morphology and wall thickness (e.g., see references 8, 9, 11, 12, 20, and 24), we expected that the hyphal wall thickness of the *ugeB*Δ strain might be similar

TABLE 1. Morphological characteristics, maximum dimension of surface subunits, and cell wall viscoelastic moduli of wild-type and Gal*f* biosynthesis enzyme gene deletion strains

Strain	Hyphal width[a] (μm) (mean ± SE)	Wall thickness[b] (nm) (mean ± SE)	Subunit maximum dimension (nm) (mean ± SD)	Viscoelastic moduli (MPa) (mean ± SD)[c] of:		Adhesion (nN) (mean ± SD)
				Fixed hyphal wall	Live hyphal wall	
Wild-type (AAE1)	2.4 ± 0.0	54 ± 2	35 ± 5	211 ± 15	82.3 ± 12.9	5.7 ± 1.6
*ugeA*Δ	3.6 ± 0.1	104 ± 10	63 ± 10	99 ± 48	24.6 ± 13.7	ND
*ugeB*Δ	2.5 ± 0.0	95 ± 11	39 ± 8	74 ± 22	22.5 ± 8.6	ND
*ugeA*Δ *ugeB*Δ	3.5 ± 0.1	217 ± 62	ND[d]	38 ± 21	9.8 ± 5.1	ND
*ugmA*Δ	3.1 ± 0.1	204 ± 10	108 ± 35	14 ± 2	3.1 ± 0.4	8.1 ± 0.3
*ugeA*Δ *ugmA*Δ	3.2 ± 0.4	162 ± 8	97 ± 23	0.05 ± 0.02	0.03 ± 0.01	17.3 ± 3.9

[a] There was no significant difference in the hyphal width for fixed or live hyphae measured by either confocal microscopy or atomic force microscopy (AFM).
[b] Measured from TEM hyphal cross sections. See Materials and Methods.
[c] Standard deviations (SDs) were calculated from the standard errors propagated through equations 1 and 2. See Materials and Methods.
[d] ND, not determined. See Results.

to that of strain AAE1. Instead, the *ugeB*Δ strain hyphal walls were almost 2-fold thicker than the hyphal walls of strain AAE1 (Table 1 and Fig. 3). Also unexpectedly, the hyphal walls of the *ugeA*Δ *ugeB*Δ double deletion strain were about twice as thick as those of either single deletion strain and even thicker than those of the *ugeA*Δ *ugmA*Δ double deletion strain (Table 1 and Fig. 3).

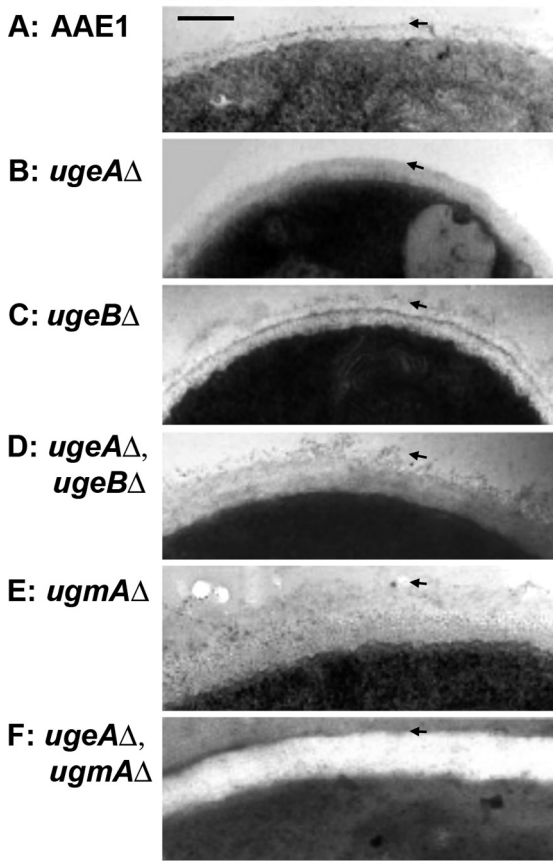

FIG. 3. Transmission electron micrographs of hyphal wall cross sections of strain AAE1 and Gal*f* biosynthesis gene deletion strains used in this study. Impressions regarding the relative hyphal diameter as assessed by curvature may be misleading, because some hyphal cross sections were not perpendicular to the hyphal axis. Images have been contrast adjusted to highlight wall structure; the cytoplasm is dark because wall carbohydrates stain poorly by transmission electron microscopy (TEM). The arrows indicate the outer boundaries of cell wall thickness measurements. All images were photographed at the same magnification. Bar = 100 nm.

TEM images of the *ugeA*Δ (see Fig. Cb in Appendix A in reference 8) and *ugeB*Δ (data not shown) strains grown in liquid shaking cultures accumulated debris, not observed for the same strains grown on dialysis tubing (Fig. 3) or for the *ugeA*Δ *ugeB*Δ double deletion strain (data not shown).

Atomic force microscopy imaging of wild-type and Gal*f* gene deletion strains. We used AFM imaging to acquire high-spatial-resolution information about the hyphal wall surfaces of two wild-type strains and four Gal*f* biosynthesis gene deletion strains. AFM imaging provides quantitative depth resolution, thus facilitating surface subunit measurements (18, 19). Our previous work demonstrated that for the wild-type strain, A28, the walls of hyphal tips and tips of lateral branches had matured by 3 μm behind the apex, at which point their surfaces resembled unbranched regions 20 μm and 40 μm behind the tip, respectively (18). To ensure that the wall surfaces were mature for all strains, we chose analysis sites that were at least 40 μm behind the hyphal tips, expecting that wall maturation might be slower in the Gal*f* biosynthesis gene deletion strains. AFM data can be collected from living or fixed cells (e.g., reference 18). We present images of fixed hyphae for comparing wall surfaces among the suite of Gal*f* biosynthesis gene deletion strains, since hyphal wall subunit size and distribution were similar to those of living cells but were more clearly defined (18).

Contact mode AFM imaging simultaneously collects topography and lateral force information. The latter represents a convolution of topography and tip-sample interactions for rough samples, thus producing relief images with more clearly defined edge features (18). High-resolution images of the hyphae from fixed wild-type strain (AAE1) and Gal*f* biosynthesis gene deletion strain (Fig. 4) show distinct differences in their surface subunit size (Table 1) and packing. The hyphae of strain AAE1 had small rounded subunits with a consistent size and even packing. In contrast, both the *ugeA*Δ and *ugmA*Δ single deletion strains had substantially larger hyphae and more variable-sized hyphal wall surface subunits than strain AAE1 and also had less organized subunit packing. The hyphal wall of the *ugeB*Δ strain most closely resembled that of strain AAE1, but with slightly elongated subunits. The hyphal surface of the *ugeA*Δ *ugeB* double deletion strain was notable in that its

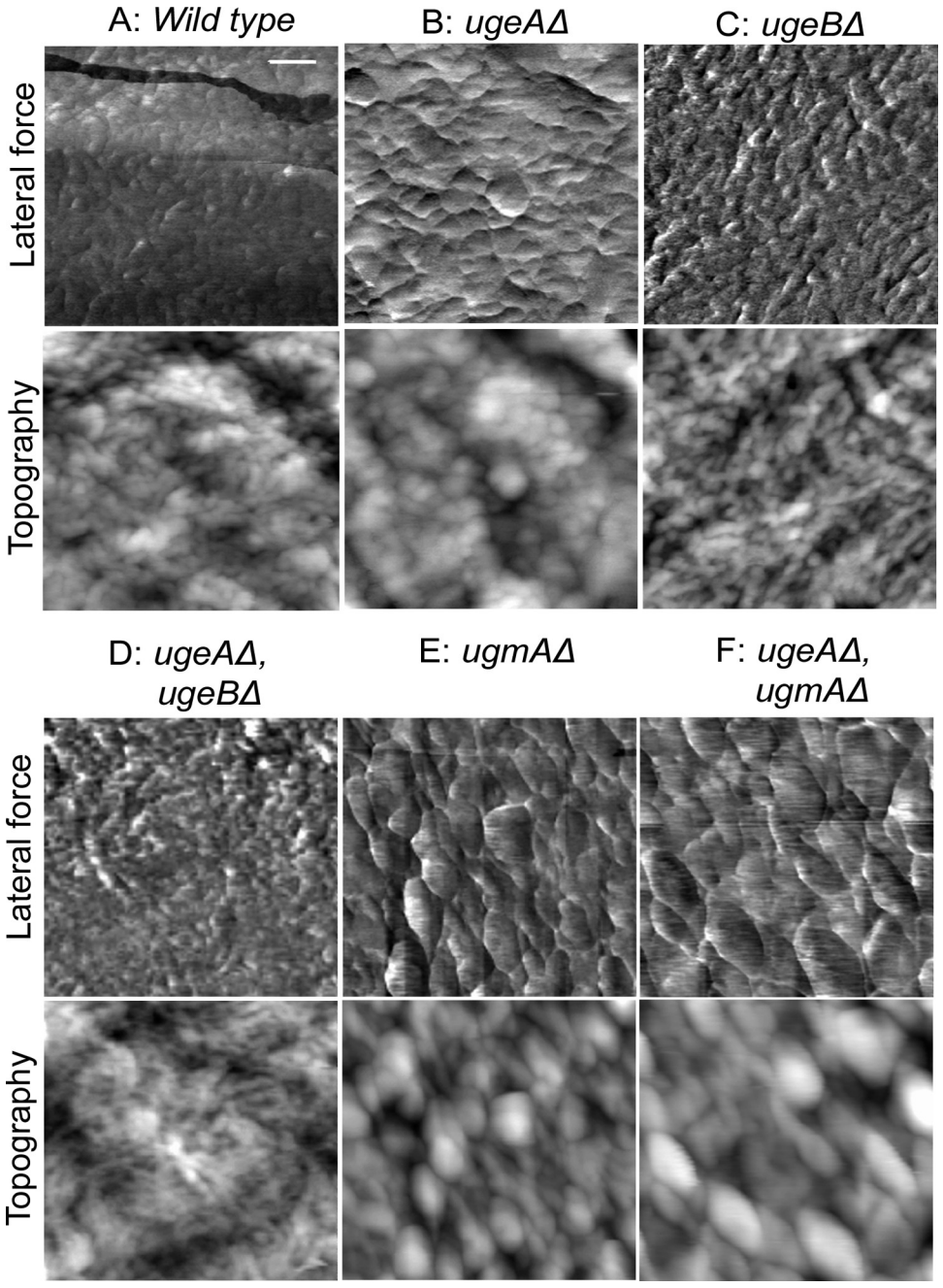

FIG. 4. Atomic force microscopy images of wild-type and Gal*f* biosynthesis gene deletion strains used in this study. The gray scale for lateral force images is ~2 nA, and for topography images, it ranges from 50 to 70 nm. All images were photographed at the same magnification. Bar = 200 nm.

surface appeared fibrillar in the topographic images; hence, maximum subunit sizes were not measured. Thus, both UgeA and UgeB appear to be important for wild-type hyphal wall surface formation. The hyphal wall surface subunits of the *ugeA*Δ *ugmA*Δ double deletion strain were similar in size to those of the *ugmA*Δ single deletion strain. Taken together, each member of the suite of Gal*f* deletion strains produced a distinctive wall phenotype.

Cell wall viscoelasticity and adhesion of wild-type and Gal*f* biosynthesis gene deletion strains. Viscoelasticity is the property describing materials such as hyphal walls, which exhibit both viscous (fluid-like) and elastic mechanical properties. Cell wall spring constants measured by FS (Fig. 5A, segment b-c) were used to calculate the viscoelastic modulus for both fixed and live hyphae of strain AAE1 and the suite of Gal*f* gene deletion strains (Table 1). Cell wall viscoelastic moduli for the single deletion strains, *ugeA*Δ and *ugeB*Δ single deletion strains, were significantly lower than that of strain AAE1 (Table 1). Viscoelastic moduli of the *ugmA*Δ single deletion strain and the double deletion strains (*ugeA*Δ *ugeB*Δ and *ugeA*Δ *ugmA*Δ) were at least an order of magnitude smaller than strain AAE1 (Table 1).

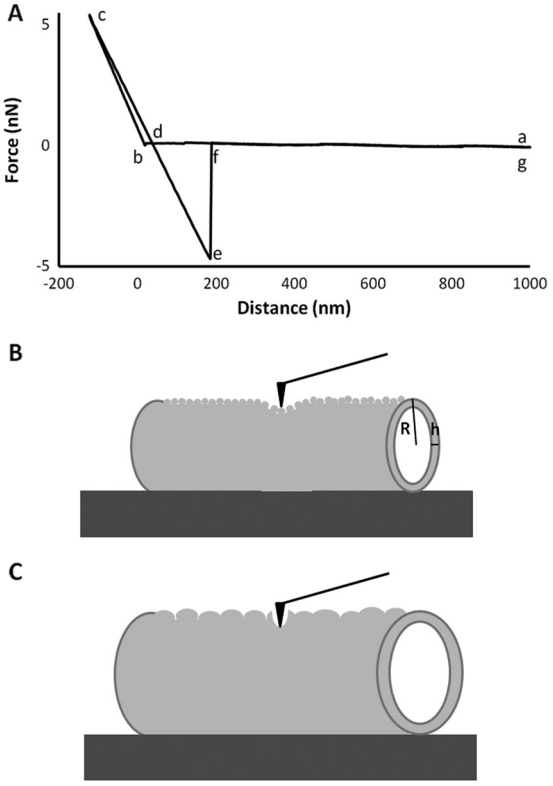

FIG. 5. (A) Representative force curve shows tip approach (a-c) with jump into contact (b) and tip retraction (c-g). The slope of segment b-c was used to calculate the sample viscoelastic modulus, and segment f-e represents tip-sample adhesion. (B and C) Schematic representations of the atomic force microscopy (AFM) tip (black) interacting with the hyphal surface (gray) of strain AEE1 and *ugeA*Δ and *ugeB*Δ single deletion strains in which the entire cell wall is deformed by tip indentation (B), compared to that of *ugmA*Δ single deletion strain and *ugeA*Δ *ugeB*Δ and *ugeA*Δ *ugmA*Δ double deletion strains in which the tip likely deforms the loosely packed, larger individual subunits or penetrates the space between subunits (C). *R* is the hyphal radius measured by TEM or AFM, and *h* is the thickness of the cell wall measured by TEM.

Notably, viscoelastic moduli of fixed hyphal walls were typically 3-fold higher than that of live ones (Table 1). Hyphal wall viscoelasticity for the suite of Gal*f* deletion strains exhibited the same trend for fixed and live hyphae.

The Si_3N_4 AFM probes used in this study have hydrophilic surfaces. We used the e-f segment of the FS curve (Fig. 5A) to quantify adhesion between *A. nidulans* wall surfaces and the AFM tip during the retraction phase. The wall surface adhesion of strain AAE1 to Si_3N_4 is shown in Table 1. The hyphae of the *ugmA*Δ single deletion strain and *ugeA*Δ *ugmA*Δ double deletion strain had significantly ($P < 0.05$) stronger adhesion to the hydrophilic tip than wild-type hyphae.

DISCUSSION

Our most notable finding is that perturbing *A. nidulans* cell wall maturation by deleting genes in the Gal*f* biosynthesis pathway has profound effects on wall surface subunit size and packing that are directly associated with cell wall viscoelasticity. This is despite the fact that none of these genes is essential for growth in culture. Previously, we used AFM and FS to show for the first time that growing hyphal tips of a wild-type *A. nidulans* strain, A28 (18), had wall surface characteristics that were consistent with long-accepted models of wall deposition and maturation (2, 26) that had yet to be quantitatively tested.

El-Ganiny et al. (8, 9) had shown using molecular biology, fluorescence microscopy, and TEM that the hyphal morphogenetic defects of the *ugeA*Δ and *ugmA*Δ deletion strains appeared to be correlated with a lack of immunolocalizable wall Gal*f* and to aberrant hyphal wall architecture. Now, we have used high-spatial-resolution AFM imaging and FS to directly quantify wall defects in this suite of Gal*f* biosynthesis gene deletion strains and to compare them to wild-type strains.

Gal*f* is required for wild-type *Aspergillus nidulans* hyphal wall formation. This AFM study is the first to make quantitative measurements of cell wall surface subunit features, wall viscoelasticity, and adhesive properties of *A. nidulans* strains that had been deleted for enzymes having roles in Gal*f* biosynthesis. Strong but circumstantial data in the study by El-Ganiny et al. (9) showed that *A. nidulans* strains lacking UgmA had defective hyphal morphogenesis, colony growth, and spore development deficits that correlated with lack of immunodetectable wall Gal*f*. Using TEM cross sections, El-Ganiny et al. (9) showed that hyphal walls of the *ugmA*Δ strain were more than four times the thickness of the hyphal walls of strain AAE1 and had poorly consolidated surfaces, suggesting that Gal*f* may play a role in wall organization.

Previously, we showed using AFM imaging that growing tips of wild-type *A. nidulans* had ellipsoidal surface subunits that were larger and more variable in size than the round subunits found 3 μm or further back (Fig. 3 in reference 18). Consistent with the decrease in subunit size and improved organization as a function of maturation, we showed an increase in surface hydrophobicity (Fig. 6D in reference 18), which was attributed to decreased exposure of sugar hydroxyl groups. El-Ganiny's study (9) suggested that the walls of the *ugmA*Δ strain were weaker than those of the wild type, since this phenotype was partially alleviated by growth on 1 M sucrose.

Our present study shows that both the *ugeA*Δ and *ugmA*Δ single deletion strains had substantially larger surface subunits than strain AAE1. In contrast, the *ugeB*Δ single deletion strain, which had wild-type colony phenotype and growth rate, had subunit sizes very similar to those of strain AAE1. Thus, it appears that *A. nidulans* surface subunit size is inversely correlated with cell wall maturation in strain A28 (18) and a suite of deletion mutants in the Gal*f* biosynthetic pathway. Our data also show that wall surface organization correlates with wall viscoelastic moduli and that these data are mirrored by the thickness and surface layer characteristics visualized in hyphal cross sections using TEM.

Viscoelastic moduli of fixed and living cell walls had a strong positive correlation, demonstrating the value of comparing fixed strains, thus reducing data collection time. The viscoelastic moduli of fixed hyphal walls were consistently larger, revealing the relationship between chemical cross-linking of the cell wall and its viscoelasticity. The data offer insight into the enzymatic cross-linking of hyphal wall components as an integral step in wall maturation, where cross-linking likely contributes to wall integrity by increasing viscoelasticity.

Strains A4 (28), A28 (18), and AAE1 (current work) are

morphological wild-type strains. The cell wall viscoelastic modulus of the fixed AEE1 strain was lower than that determined for fixed, rehydrated A4 by Zhao and coworkers (28). Although both studies used the same method to determine cantilever spring constants (5), it is only an estimate and can account for the difference in viscoelastic moduli. The viscoelastic modulus of live AEE1 cell walls (Table 1) was lower than that reported previously for A28 (115 ± 31 MPa; 18). However, since the latter study compared viscoelastic moduli in different regions along single hyphae, cantilevers were not calibrated.

We used Zhao's model (18), which assumes the indentation of a contiguous layer (cell wall) surrounding a large cylinder (hyphae; Fig. 5B), to calculate cell wall viscoelastic moduli. A plot of the dimensionless unit Eh/k_w versus $(R/h)^{1.5}$ (data not shown) suggests that this model fits strain AEE1 and *ugeA*Δ and *ugeB*Δ single deletion strains better than it does the poorly ordered walls of the *ugmA*Δ single deletion strain and the *ugeA*Δ *ugeB*Δ and *ugeA*Δ *ugmA*Δ double deletion strains. Differences can at least in part be attributed to the composition and organization of cell wall components (Fig. 5B), whereas the viscoelastic modulus data for the *ugmA*Δ single deletion strain and *ugeA*Δ *ugeB*Δ and *ugeA*Δ *ugmA*Δ double deletion strains suggest that the AFM tip may penetrate the loosely packed cell wall surface. The Si_3N_4 AFM tips used in this study have tips that are about 10 nm wide (18). The subunits of the *ugmA*Δ and *ugeA*Δ *ugmA*Δ strains are 10-fold larger (Table 1), so the AFM tip could possibly pierce an individual subunit. The surface of the *ugeA*Δ *ugeB*Δ strain has a fibrillar appearance (Fig. 5C), so its interaction with the AFM tip could be unlike the other deletion strains we studied.

Gal*f* appears to mediate *Aspergillus nidulans* hyphal wall surface and hyphal adhesion. Lamarre et al. (14) suggested that hyphal wall Gal*f* plays a role in *A. fumigatus* hyphal wall surface properties, which they showed qualitatively by the accumulation of material on *Afugm1*Δ hyphal walls using scanning electron microscopy (SEM) and by hyphal adhesion to substrates, including glass and plastic coverslips, latex beads, and epithelial respiratory cells.

We quantified the adhesion between the hydrophilic Si_3N_4 AFM tip and walls of living hyphae of strain AAE1, the *ugmA*Δ single deletion strain, and the *ugeA*Δ *ugmA*Δ double deletion strain. The increasing hyphal wall surface disorder in *ugmA*Δ and *ugeA*Δ *ugmA*Δ deletion strains correlates with effects on hyphal wall viscoelasticity and adhesion. The loose packing of hyphal wall surfaces observed by AFM imaging of Gal*f* mutants would expose polar groups normally masked during wall maturation, increasing hydrophilic character of the wall surface and resulting in greater adhesion. Consistent with the results of Lamarre et al. (14), the *ugmA*Δ single deletion strain and the *ugeA*Δ *ugmA*Δ double deletion strain tended to adhere to microscope coverslips compared to strain AAE1 and the *ugeB*Δ single deletion strain (data not shown). The adhesion values between the Si_3N_4 tip and the walls of *ugmA*Δ and *ugeA*Δ *ugmA*Δ deletion strains were comparable to those previously reported for A28 hyphae at growing tips, where the wall is newly deposited and not yet mature (~9 nN [18]). Thus, surface subunit size, wall viscoelasticity, and wall adhesion to hydrophilic surfaces show consistent trends for wild-type and Gal*f* gene deletion strains.

Schmalhorst et al. (23) provided data to suggest that the *A. fumigatus glfA*Δ (homologous to *A. nidulans ugmA* [9]) strain had attenuated virulence in a murine model for systemic aspergillosis. However, scanning electron microscopy of cross-fractured *glfA*Δ hyphal walls were half the thickness of wild-type *A. fumigatus* walls, the opposite trend to our study that deserves further attention.

By combining gene deletion characterizations with TEM, AFM, and FS, we have shown that Gal*f* is important for *A. nidulans* hyphal wall maturation. However, despite the strong correlation between our results and those of Lamarre et al. (14) we are not yet able to determine the likely location(s) of Gal*f*-containing molecules in *A. nidulans* walls. Indeed, Latgé's 2010 model (16) discusses these molecules without indicating many details relating to their deployment in the three-dimensional wall architecture.

We have shown that perturbing wild-type Gal*f* cell wall deposition has substantial effects on the surface ultrastructure and viscoelasticity of the *Aspergillus nidulans* cell wall. Gal*f* appears to have crucial and multiple roles in *Aspergillus* hyphal cell wall maturation and integrity. Studies addressing potential roles of mannose in *A. nidulans* wall structure and adhesive properties and potential roles of Gal*f* in pathogenicity are under way.

ACKNOWLEDGMENTS

This research was supported by Natural Science and Engineering Research Council of Canada Discovery grants to T.E.S.D. and S.G.W.K., a Canadian Institutes of Health Research/Regional Partnership Program grant to S.G.W.K., and by an Egyptian Ministry of Higher Education grant to A.M.E.-G. B.C.P. was partially supported by the Department of Chemistry and Biochemistry, Faculty of Science, University of Regina.

REFERENCES

1. **Bar-Peled, M., C. L. Griffith, J. J. Ory, and T. L. Doering.** 2004. Biosynthesis of UDP-GlcA, a key metabolite for capsular polysaccharide synthesis in the pathogenic fungus *Cryptococcus neoformans*. Biochem. J. **381:**131–136. doi:10.1042/BJ20031075.
2. **Bartnicki-Garcia, S., C. E. Bracker, G. Gierz, R. Lopez-Franco, and H. Lu.** 2000. Mapping the growth of fungal hyphae: orthogonal cell wall expansion during tip growth and the role of turgor. Biophys. J. **79:**2382–2390. doi:10.1016/S0006-3495(00)76483-6.
3. **Beverley, S. M., et al.** 2005. Eukaryotic UDP-galactopyranose mutase (*GLF* gene) in microbial and metazoal pathogens. Eukaryot. Cell **4:**1147–1154. doi:10.1128/EC.4.6.1147-1154.2005.
4. **Cappella, B., and G. Dietler.** 1999. Force-distance curves by atomic force microscopy. Surf. Sci. Rep. **34:**5–104.
5. **Cleveland, J. P., and S. Manne.** 1993. A nondestructive method for determining the spring constant of cantilevers for scanning probe microscopy. Rev. Sci. Instrum. **64:**403–405.
6. **Damveld, R. A.** 2008. A novel screening method for cell wall mutants in *Aspergillus niger* identifies UDP-galactopyranose mutase as an important protein in fungal cell wall biosynthesis. Genetics **178:**873–881.
7. **de Groot, P. W., et al.** 2009. Comprehensive genomic analysis of cell wall genes in *Aspergillus nidulans*. Fungal Genet. Biol. **46**(Suppl. 1)**:**S72–S81.
8. **El-Ganiny, A. M., I. Sheoran, D. A. R. Sanders, and S. G. W. Kaminskyj.** 2010. *Aspergillus nidulans* UDP-glucose-4-epimerase UgeA has multiple roles in wall architecture, hyphal morphogenesis, and asexual development. Fungal Genet. Biol. **47:**629–635. doi:10.1016/j.fgb.2010.03.002.
9. **El-Ganiny, A. M., D. A. R. Sanders, and S. G. W. Kaminskyj.** 2008. *Aspergillus nidulans* UDP-galactopyranose mutase, encoded by *ugmA* plays key roles in colony growth, hyphal morphogenesis, and conidiation. Fungal Genet. Biol. **45:**1533–1542. doi:10.1016/j.fgb.2008.09.008.
10. **Gastebois, A.** 2009. *Aspergillus fumigatus*: cell wall polysaccharides, their biosynthesis and organization. Future Microbiol. **4:**583–595.
11. **Harris, S. D.** 2009. Morphology and development in *Aspergillus nidulans*: a complex puzzle. Fungal Genet. Biol. **46**(Suppl. 1)**:**S82–S92.
12. **Kaminskyj, S. G. W., and J. E. Hamer.** 1998. *hyp* loci control cell pattern formation in the vegetative mycelium of *Aspergillus nidulans*. Genetics **148:**669–680.

13. **Kaminskyj, S. G. W.** 2001. Fundamentals of growth, storage, genetics and microscopy of *Aspergillus nidulans*. Fungal Genet. Newsl. **48:**25–31.
14. **Lamarre, C., et al.** 2009. Galactofuranose attenuates cellular adhesion of *Aspergillus fumigatus*. Cell. Microbiol. **11:**1612–1623.
15. **Latgé, J.-P.** 2009. Galactofuranose containing molecules in *Aspergillus fumigatus*. Med. Mycol. **47**(Suppl. 1)**:**S104–S109. doi:10.1080/13693780802258832.
16. **Latgé, J.-P.** 2010. Tasting the fungal cell wall. Cell. Microbiol. **12:**863–872. doi:10.1111/j.1462-5822.2010.01474.x.
17. **Lesage, G., and H. Bussey.** 2006. Cell wall assembly in *Saccharomyces cerevisiae*. Microbiol. Mol. Biol. Rev. **70:**317–343.
18. **Ma, H., L. A. Snook, S. G. W. Kaminskyj, and T. E. S. Dahms.** 2005. Surface ultrastructure and elasticity in growing tips and mature regions of *Aspergillus* hyphae describe wall maturation. Microbiology **151:**3679–3688. doi:10.1099/mic.0.28328-0.
19. **Ma, H., L. A. Snook, C. Tian, S. G. W. Kaminskyj, and T. E. S. Dahms.** 2006. Fungal surface remodelling visualized by atomic force microscopy. Mycol. Res. **110:**879–886. doi:10.1016/j.mycres.2006.06.010.
20. **Momany, M., P. J. Westfall, and G. Abramowsky.** 1999. *Aspergillus nidulans* swo mutants show defects in polarity establishment, polarity maintenance and hyphal morphogenesis. Genetics **151:**557–567.
21. **Moyrand, F., I. Lafontaine, T. Fontaine, and G. Janbon.** 2008. UGE1 and UGE2 regulation of the UDP-glucose/UDP-galactose equilibrium in *Cryptococcus neoformans*. Eukaryot. Cell **7:**2069–2077.
22. **Perfect, J. R.** 2005. Nuances of new anti-*Aspergillus* antifungals. Med. Mycol. **43**(Suppl. 1)**:**S271–S276.
23. **Schmalhorst, P. S., et al.** 2008. Contribution of galactofuranose to the virulence of the opportunistic pathogen *Aspergillus fumigatus*. Eukaryot. Cell **7:**1268–1277. doi:10.1128/EC.00109-08.
24. **Shi, X., Y. Sha, and S. G. W. Kaminskyj.** 2004. *Aspergillus nidulans hypA* regulates morphogenesis through the secretion pathway. Fungal Genet. Biol. **41:**75–88.
25. **Wallis, G. L., F. W. Hemming, and J. F. Peberdy.** 2001. Beta-galactofuranoside glycoconjugates on conidia and conidiophores of *Aspergillus niger*. FEMS Microbiol. Lett. **201:**21–27.
26. **Wessels, J. G.** 1999. Fungi in their own right. Fungal Genet. Biol. **27:**134–145. doi:10.1006/fgbi.1999.1125.
27. **Xu, S., and M. F. Arnsdorf.** 1994. Calibration of the scanning (atomic) force microscope with gold particles. J. Microsc. **173:**199–210.
28. **Zhao, L., et al.** 2005. Elastic properties of the cell wall of *Aspergillus nidulans* studied with atomic force microscopy. Biotechnol. Prog. **21:**292–299.